

# Variations of spectral signature profiles of wet and dry targets for supporting the detection of water-leakages using satellite data

Athos Agapiou\*<sup>a</sup>, Kyriacos Themistocleous<sup>a</sup>, Dimitrios D. Alexakis<sup>a</sup>, Nikolas Kourtis<sup>a</sup>, Apostolos Sarris<sup>b</sup>, Skevi Perdikou<sup>c</sup>, Chris R.I. Clayton<sup>d</sup>, Helena Phinikaridou<sup>e</sup>, Andreas Manoli<sup>e</sup>, Diofantos G. Hadjimitsis<sup>a</sup>

<sup>a</sup>Department of Civil Engineering and Geomatics, Remote Sensing and Geo-Environment Lab, School of Engineering and Technology Cyprus University of Technology, 2-8 Saripolou, 3036 Lemesos, Cyprus

<sup>b</sup>Laboratory of Geophysical-Satellite Remote Sensing & Archaeoenvironment, Institute for Mediterranean Studies, Foundation for Research & Technology-Hellas (F.O.R.T.H.), Nik. Foka 130, Rethymno, 74100, Crete, Greece

<sup>c</sup>Frederick Research Centre, Filokyprou 7-9, Pallouriotissa, Nicosia;

<sup>d</sup>Southampton University, Faculty of Engineering and the Environment, Highfield, Southampton

<sup>e</sup>Water Development Department, 100-110 Kennenty Aven., 1047 Pallouriotissa, Lefkosia

## ABSTRACT

Satellite data can be used as a valuable tool for the detection of water pipeline leakages in semiarid areas. However the use of multi-temporal satellite images for this purpose can be problematic since reflectance values may change due to phenological changes of plants, radiometric errors during the pre-processing of satellite data, etc. It is therefore important to establish a spectral signature library with “ground truth data” for different scenarios of water leakages in a control site minimizing other potential errors. For this purpose, the GER 1500 spectroradiometer was used for measuring the reflectance values of three different targets: soil, vegetation and asphalt. The targets were saturated with a specific amount of water and then several spectroradiometric measurements were taken. The narrowband reflectance values were then re-scaled to spectral bands of Landsat 5 TM and spectral signature variations were highlighted for all targets before and after moisture level were increased. Using these data, threshold values were defined in order to be used for multispectral satellite data analysis. Specifically, this data was used for detection of water leakages in pipelines in Cyprus using Landsat 5 TM images,.

**Keywords:** water leakages, remote sensing, ground spectroscopy, spectral library, dry and wet targets.

## 1. INTRODUCTION

Reduction of water leakages is an important goal in different countries in the world [1]. Especially in the Mediterranean region, droughts have increased dramatically during the last decades. Optimizing water distribution systems and water saving measurements are some actions taken by local authorities to minimize water losses. Much publicity has surrounded the issue of water leakages as well as monitoring water pipes using different sensors and technologies. According to Pickerell and Malthus [2], leakage is related to economic loss, customer inconvenience and severe environmental impacts.

During the last decades, remote sensing has played an increasing role in the field of hydrology, especially water management [3]. It is considered that the resolution in time and space of remotely sensed data is vital in water management [4]. The latter is true in case of early warning systems for the detection of water leakages. According to Tasumi et al [5], the use of remotely sensed data is very useful for the deployment of water strategies because it can offer a vast amount of information in short time, compared to conventional methods. Remotely sensed data provides a quick, convenient and less expensive tool for data acquisition, especially in an extended area.

Preliminary results for the detection of leakages in semi-arid environment have been evaluated in the region of Cyprus [6]. The results have shown that different remote sensing technologies can be applied for the detection and monitoring of

water leakages for water utility systems located in open fields in Cyprus. According to Agapiou et al [6], two case study areas were evaluated using freely distributed Landsat 7 ETM+ satellite images and ground spectroradiometric data. In addition, a low altitude system was deployed to observe these pipelines from different heights (Figure 1). The low altitude system was used to verify the detection of leakages, as presented in the Landsat 7 ETM+ satellite images.

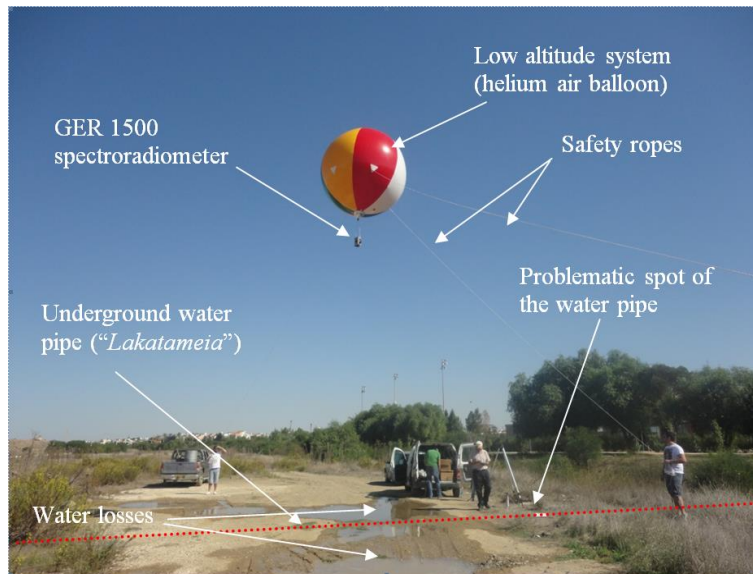


Figure 1. A low altitude system deployed over the leakage in an underground waterpipe [6].

This paper aims to identify thresholds, for reflectance and vegetation indices (VIs) as well as to create spectral libraries for several targets in order to improve the detection of leakages using satellite data and assist the final user. For this reason, the GER 1500 ground spectroradiometer was used and several ground truth reflectance values were recorded. Appropriate Relative Spectral Response (RSR) filters of the Landsat 7 ETM+ were used to calculate the broadband reflectance. In addition, several VIs were calculated and the threshold values were determined. Finally, a ‘created’ water leakage was detected using both medium and high resolution satellite images.

## 2. MATERIALS AND METHODS

### 2.1 Ground Spectroradiometer

Spectroradiometric hyperspectral measurements were carried out using the GER 1500 field spectroradiometer. The GER 1500 spectroradiometer records electromagnetic radiation between 350 nm to 1050 nm (visible and near infrared part of the spectrum) A calibrated spectralon panel, with  $\approx 100\%$  reflectance, was also used simultaneously to measure the incoming solar radiation. The spectralon panel measurement was used as a reference [7].

Hyperspectral measurements recorded from the GER 1500 instrument needed to be recalculated according to the characteristics of a specific multispectral satellite sensor. The hyperspectral measurements from the Landsat 7 ETM+ satellite imagery were upscaled with the Relative Spectral Response (RSR) filters. RSR filters describe the instrument relative sensitivity to radiance in various parts of the electromagnetic spectrum [8]. These spectral responses values range from 0 to 1 and have no units since they are relative to the peak response (Figure 2). RSR filters are used in the same way in spectroradiometers in order to transmit a certain wavelength band and block others. The reflectance from the spectroradiometer was calculated based on the wavelength of each sensor and the RSR filter as follows:

$$R_{band} = \frac{\sum (R_i * RSR_i)}{\sum RSR_i} \quad (1)$$

Where:

$R_{band}$  = reflectance at a range of wavelength (e.g. Band 1)

Ri = reflectance at a specific wavelength (e.g R 450 nm)

RSRi = Relative Response value at the specific wavelength

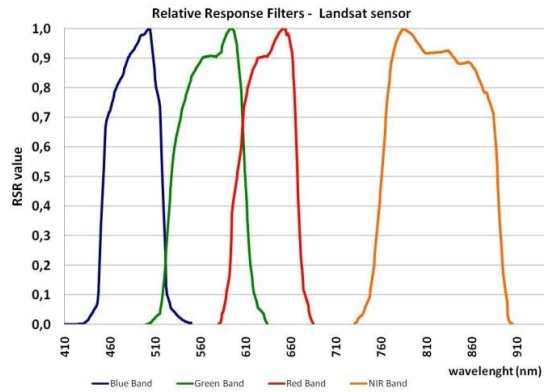


Figure 2. Relative Response filters for Bands 1-4 of Landsat TM sensor [6]

The broadband reflectance was then used in order to calculate several VIs as shown in Table 1 [9]. In addition to widely used vegetation indices, such as the NDVI, other indices were also examined in order to evaluate their performance for the detection of water leakages. False composites were also examined using a QuickBird and ALOS –AVNIR-2 images.

Table 1: Vegetation indices used in this study [9].

no	Vegetation Index	Equation
1	EVI (Enhanced Vegetation Index)	$2.5 (p_{NIR} - p_{red}) / (p_{NIR} + 6 p_{red} - 7.5 p_{blue} + 1)$
2	Green NDVI (Green Normalized Difference Vegetation Index)	$(p_{NIR} - p_{green}) / (p_{NIR} + p_{green})$
3	NDVI (Normalized Difference Vegetation Index)	$(p_{NIR} - p_{red}) / (p_{NIR} + p_{red})$
4	SR (Simple Ratio)	$p_{NIR} / p_{red}$
5	MSR (Modified Simple Ratio)	$p_{red} / (p_{NIR} / p_{red} + 1)^{0.5}$
6	MTVI2 (Modified Triangular Vegetation Index)	$[1.5(1.2*(p_{NIR} - p_{green}) - 2.5(p_{red} - p_{green})) / [(2 p_{NIR} + 1)^2 - (6 p_{NIR} - 5 p_{red}^{0.5}) - 0.5]^{0.5}]$
7	RDVI (Renormalized Difference Vegetation Index)	$(p_{NIR} - p_{red}) / (p_{NIR} + p_{red})^{1/2}$
8	IRG (Red Green Ratio Index)	$p_{red} - p_{green}$
9	PVI (Perpendicular Vegetation Index)	$(p_{NIR} - \alpha p_{red} - b) / (1 + \alpha^2)$ $p_{NIR,soil} = \alpha p_{red,soil} + b$
10	RVI (Ratio Vegetation Index)	$p_{red} / p_{NIR}$
11	TSAVI (Transformed Soil Adjusted Vegetation Index)	$[\alpha(p_{NIR} - \alpha p_{red} - b)] / [(p_{red} + \alpha p_{NIR} - \alpha b + 0.08(1 + \alpha^2))]$ $p_{NIR,soil} = \alpha p_{red,soil} + b$

12	MSAVI (Modified Soil Adjusted Vegetation Index)	$[2 p_{NIR}+1-[(2 p_{NIR}+1)^2-8(p_{NIR} - p_{red})]^{1/2}]/ 2$
13	ARVI (Atmospherically Resistant Vegetation Index)	$(p_{NIR} - p_{rb})/(p_{NIR} + p_{rb}),$ $p_{rb} = p_{red} - \gamma (p_{blue} - p_{red})$
14	GEMI (Global Environment Monitoring Index)	$n(1-0.25n)(p_{red} - 0.125)/(1 - p_{red})$ $n = [2(p_{NIR}^2 - p_{red}^2)+1.5 p_{NIR}+0.5 p_{red}] / (p_{NIR}+ p_{red}+0.5)$
15	SARVI (Soil and Atmospherically Resistant Vegetation Index)	$(1+0.5)(p_{NIR} - p_{rb})/(p_{NIR} + p_{rb}+0.5)$ $p_{rb} = p_{red} - \gamma (p_{blue} - p_{red})$
16	OSAVI (Optimized Soil Adjusted Vegetation Index)	$(p_{NIR} - p_{red}) / (p_{NIR} + p_{red} + 0.16)$
17	DVI (Difference Vegetation Index)	$p_{NIR} - p_{red}$
18	SR × NDVI (Simple Ratio × Normalized Difference Vegetation Index)	$(p_{NIR}^2 - p_{red}^2) / (p_{NIR} + p_{red}^2)$

## 2.2 Case study areas

Three different targets were examined for the purpose of this paper: soil; vegetation and asphalt. These targets were selected since both soil and vegetation cover the majority of the semi-arid water network of our case study (Cyprus). In addition, asphalt was also examined, since water leakages might be observed in areas where the underground pipeline crosses rural roads. The campaign was performed in an arid agricultural area in the Limassol district, Cyprus.



Figure 3. The different targets examined in this paper. From left to right: vegetation; asphalt and soil.

Nearly 200 ground measurements were taken over these three different targets under clear sky conditions. The targets were saturated with different amount of water each time while spectroradiometric measurements were recorded each time. In this way, the change of reflectance value compared with the water saturation amount was examined.

## 3. RESULTS

In this section the results from the above fieldwork and application to high resolution satellite data is presented. The reflectance values for each different target is presented in relation with the wavelength and the moisture, as well an evaluation of the VIs examined in this paper (see Table 1).

### 3.1 Reflectance Values

As expected, wet soil have lower reflectance values than the dry condition in the whole part of the spectrum examined in this paper (visible – very near infrared part of the spectrum). Indeed, as shown in Figure 4, reflectance values are reduced with a minimum amount of water ( $\approx 0.3 \text{ mm} / \text{cm}^2$ ). Reflectance values then increased ( $\approx 0.6 - 1.25 \text{ mm} / \text{cm}^2$ ), but the reflectance values are still lower in the visible and very near infrared bands than the dry conditions. Higher reflectance values are finally observed in the last experiment ( $\approx 2 \text{ mm} / \text{cm}^2$ ) due to reflectance of the remaining water over the soil target.

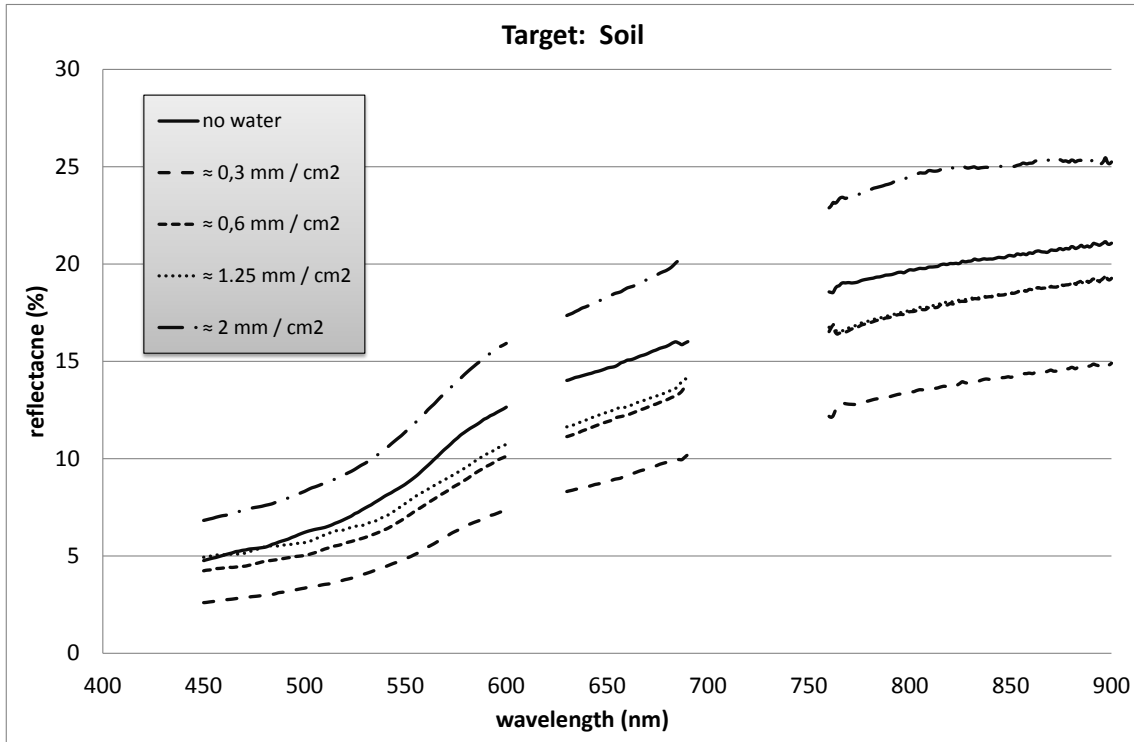


Figure 4. Mean spectral signature profiles for vegetation in different moisture levels.

The mean reflectance values for the visible and very near infrared part of the spectrum are shown in Table 2. The standard deviation for the dataset is less than 1% (with some exceptions). Maximum reflectance difference between the dry and wet soil is observed in the beginning of the experiment ( $\approx 0.3 \text{ mm} / \text{cm}^2$ ) and then when the water remains over the surface ( $\approx 2 \text{ mm} / \text{cm}^2$ ). This observation indicates that detection of leakage over soil can be detected using remote sensing techniques either in the early beginning of the leakage (i.e. when the soil surface gets wet) or when the leakage is not fixed and the water remains over the soil. The red and VNIR part of the spectrum seems to be the most promising to detect any leakage since at this spectral range the reflectance is decreased by 35-40% for the dry soil.

Table 2: Reflectance values (%) of the soil target for the visible and near infrared part of the spectrum.

Moisture level	no water	$\approx 0,3 \text{ mm} / \text{cm}^2$	$\approx 0,6 \text{ mm} / \text{cm}^2$	$\approx 1 \text{ mm} / \text{cm}^2$	$\approx 1.25 \text{ mm} / \text{cm}^2$	$\approx 2 \text{ mm} / \text{cm}^2$
<b>Blue</b>	$5.73 \pm 0.61$	$3.11 \pm 0.34$	$4.82 \pm 0.41$	$5.14 \pm 0.41$	$5.52 \pm 0.42$	$7.85 \pm 0.69$
<b>Green</b>	$9.69 \pm 1.80$	$5.48 \pm 1.13$	$7.70 \pm 1.41$	$7.91 \pm 1.34$	$8.37 \pm 1.38$	$12.45 \pm 2.12$
<b>Red</b>	$15.04 \pm 0.63$	$9.18 \pm 0.56$	$12.29 \pm 0.71$	$12.13 \pm 0.64$	$12.74 \pm 0.68$	$18.78 \pm 0.86$
<b>VNIR</b>	$20.07 \pm 0.67$	$13.85 \pm 0.70$	$18.04 \pm 0.83$	$17.26 \pm 0.76$	$18.09 \pm 0.78$	$24.69 \pm 0.65$

Spectral signatures of different moisture levels for vegetation target are shown Figure 5. The average and standard deviation of the measurements are presented in Table 3. The results indicate that early detection of leakage, regardless of the moisture level, may be problematic since it is difficult to distinguish dry and wet vegetation. However, variations in the phenological cycle of crops or the appearance of vegetation over wet soil after a short period are expected and these can be easily tracked using change detection techniques. These observations were not analyzed in the field experiment.

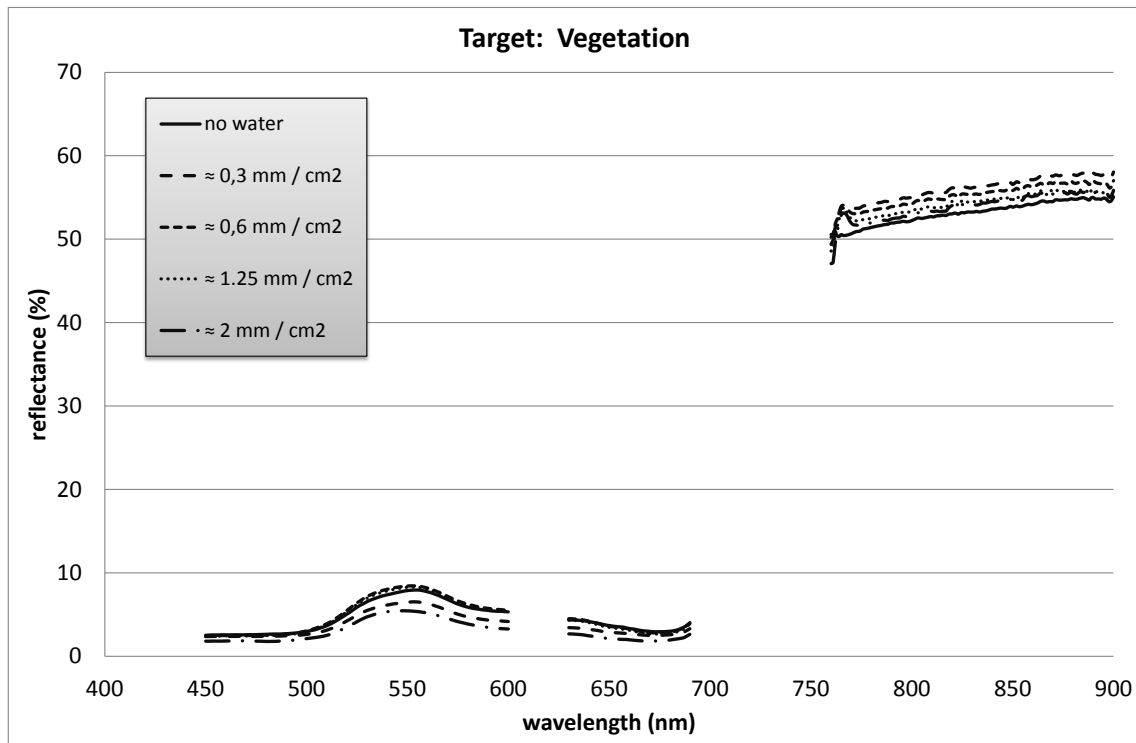


Figure 5. Mean spectral signature profiles for vegetation with different moisture levels.

Table 3: Reflectance values (%) of the vegetation target for the visible and near infrared part of the spectrum.

Moisture level	no water	≈ 0,3 mm / cm <sup>2</sup>	≈ 0,6 mm / cm <sup>2</sup>	≈ 1 mm / cm <sup>2</sup>	≈ 1.25 mm / cm <sup>2</sup>	≈ 2 mm / cm <sup>2</sup>
<b>Blue</b>	2,97 ± 0.65	2,65 ± 0.47	3,00 ± 0.80	2,98 ± 0.72	2,92 ± 0.76	2,07 ± 0.43
<b>Green</b>	6,60 ± 0.94	5,39 ± 0.83	7,05 ± 1.04	6,75 ± 1.02	6,88 ± 1.04	4,48 ± 0.77
<b>Red</b>	3,53 ± 0.49	2,86 ± 0.31	3,48 ± 0.57	3,32 ± 0.51	3,34 ± 0.56	2,14 ± 0.28
<b>VNIR</b>	53,11 ± 1.41	55,97 ± 1.55	55,18 ± 1.40	54,48 ± 1.33	54,23 ± 1.38	53,86 ± 1.58

Asphalt was the last target of the field experiment. The results show that wet asphalt of any level of moisture can be detected using remote sensing techniques (Figure 6; Table 4). The reflectance values for wet asphalt can be less than 3.5% in the VNIR part of the spectrum and less than 2.5% for the visible part of spectrum.

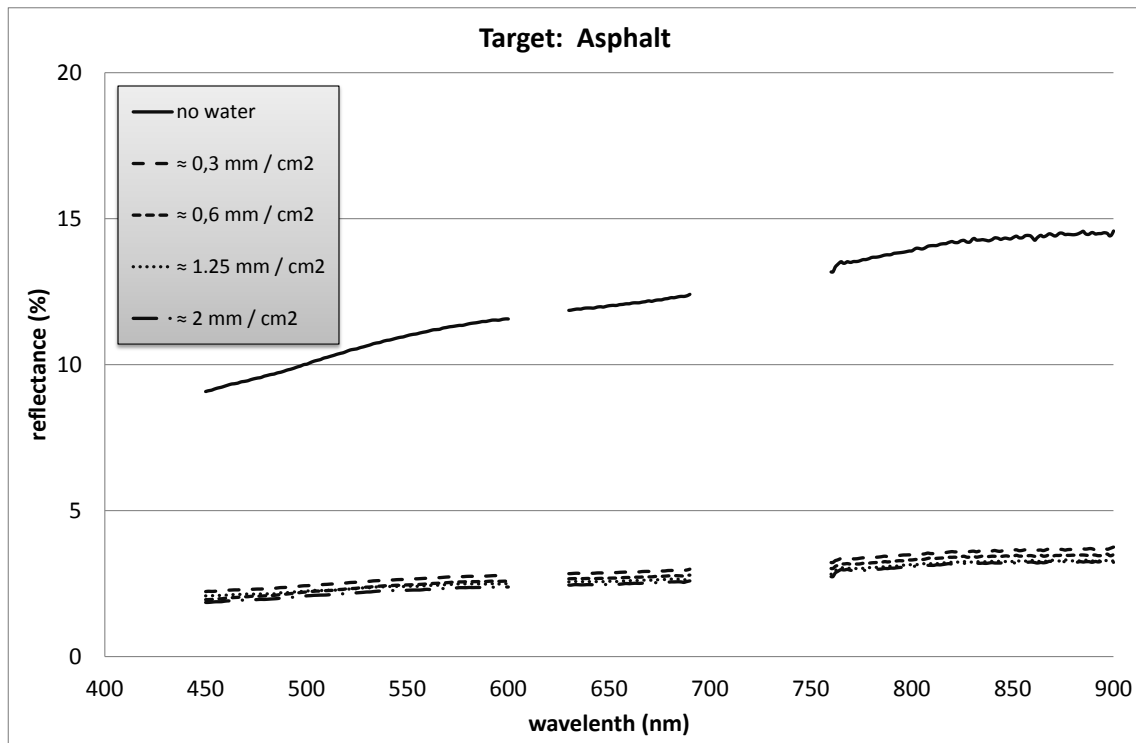


Figure 6. Mean spectral signature profiles for asphalt in different moisture levels.

Table 4: Reflectance values (%) of the vegetation target for the visible and near infrared part of the spectrum.

Moisture level	no water	≈ 0,3 mm / cm <sup>2</sup>	≈ 0,6 mm / cm <sup>2</sup>	≈ 1 mm / cm <sup>2</sup>	≈ 1.25 mm / cm <sup>2</sup>	≈ 2 mm / cm <sup>2</sup>
Blue	9,74 ± 0.40	2,36 ± 0.09	2,12 ± 0.11	2,02 ± 0.07	2,18 ± 0.07	2,00 ± 0.09
Green	11,10 ± 0.33	2,67 ± 0.07	2,48 ± 0.08	2,27 ± 0.06	2,43 ± 0.05	2,29 ± 0.06
Red	12,10 ± 0.15	2,90 ± 0.04	2,71 ± 0.04	2,47 ± 0.04	2,60 ± 0.03	2,50 ± 0.04
VNIR	14,12 ± 0.35	3,55 ± 0.12	3,36 ± 0.11	3,07 ± 0.11	3,19 ± 0.11	3,14 ± 0.11

From the previous results, it is shown that with minimum moisture level the leakage is able to be detected in both soil and asphalt targets. Areas covered with vegetation can be problematic since multi-temporal analysis is required to verify the results. The evaluation of several broadband indices also been examined based in the above reflectance values.

### 3.2 Vegetation Indices

The purpose of this analysis was to evaluate different broadband vegetation indices (see Table 1) for the detection of water leakages. In addition, quantification of the results was also applied. The indices were calculated based on the reflectance values of ground spectral signatures for the Landsat sensor. Figures 7-9 present the relative difference of several vegetation indices compared to the dry conditions. In detail Figure 7 shows the results for soil; Figure 8 for vegetation and Figure 9 for asphalt.

As shown, some vegetation indices tend to maximize the difference observed between wet and dry conditions. In addition it was found that no unique index is suitable for all different case studies. For soil target the MTVI2 index tends to give the higher contrast between the beginning of the leakage and the dry soil. The relative difference has been estimated to nearly 200%. TSAVI is another promising index; since the relative difference is more than 150% TSAVI index might be used in vegetated areas with low Leaf Area Index (LAI) in order to minimize the soil background effect. In general all indices revealed that during the beginning of a leakage tend to give contrast from 10% - nearly 200%.

More complicated seems to be the results for the vegetation target. In general the relative difference is less than 20% for all indices and for all different levels of moisture. GEMI index gave the highest values for the vegetation target. Finally,

regarding asphalt target, several indices have been able to enhance the contrast between dry and wet target with more than 100%. Again MTIVI2 as well as GEMI shows high difference values (nearly 300%).

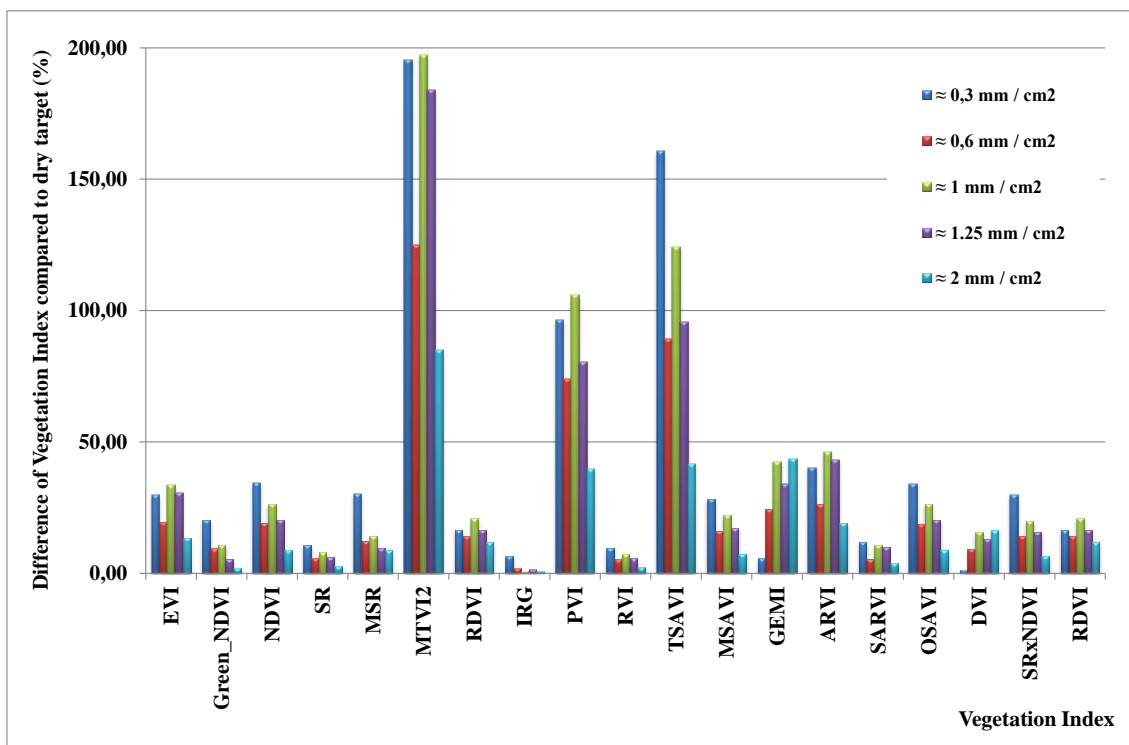


Figure 7: Relative difference of vegetation indices of wet soil compared to the dry soil.

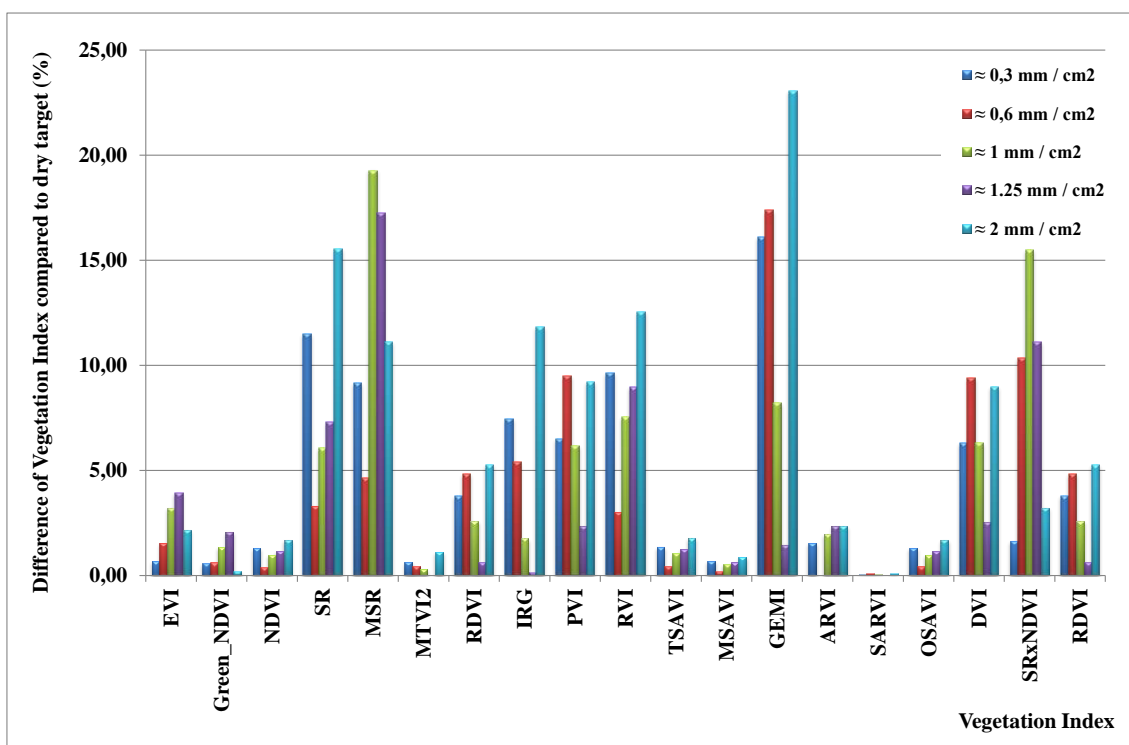


Figure 8: Relative difference of vegetation indices of wet soil compared to the dry vegetation.

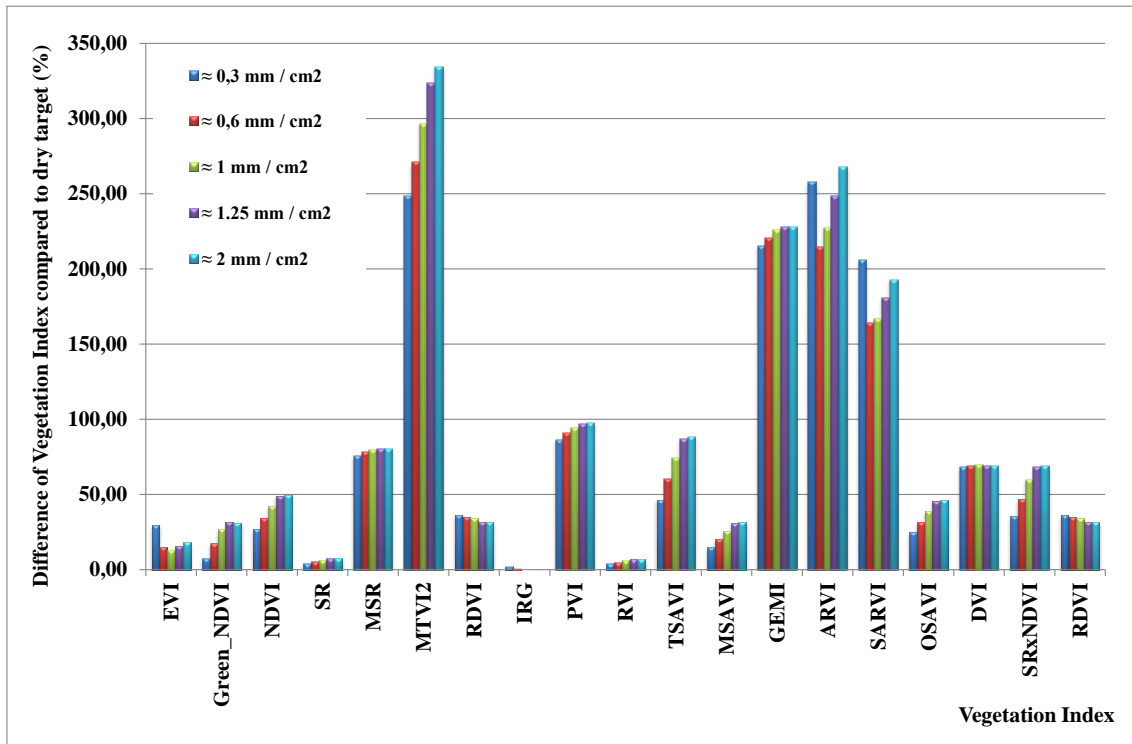


Figure 9: Relative difference of vegetation indices of wet soil compared to the dry asphalt.

### 3.3 High and medium resolution satellite image for the detection of known leakage

An identified water leakage was examined using high and medium resolution satellite image (QuickBird and ALOS - AVNIR-2) in the Pyla area (central Cyprus). The pipeline of the area was imported in the ArcGIS software. A buffer zone of 100 meter around the pipeline was also created to minimize the area of interest, as indicated in Figure 10. The QuickBird image with overpass of 07 July 2007 was acquired only a few days before the pipeline was fixed from the local authorities. The same date (07 July 2007) the ALOS -AVNIR-2 image was also acquired.

The results from the ALOS -AVNIR-2 (10 m spatial resolution) as shown in Figure 11, indicate a linear vegetated area in the same direction of the buried pipeline. Vegetated area has been detected in the ALOS image indicating an unusual event. During this period, the rainfall was 0.0 mm while July is generally considered one of the hottest months of the year in Cyprus. A better interpretation can be viewed using the high resolution satellite QuickBird image (Figure 12).

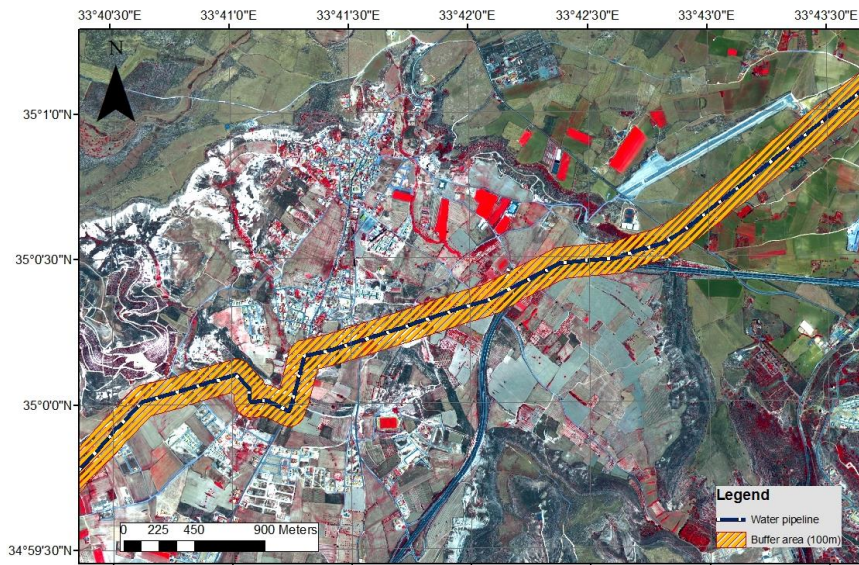


Figure 10: QuickBird satellite image over the Pyla area in central Cyprus. The image was taken a few days before local authorities fixed the leakage problem.

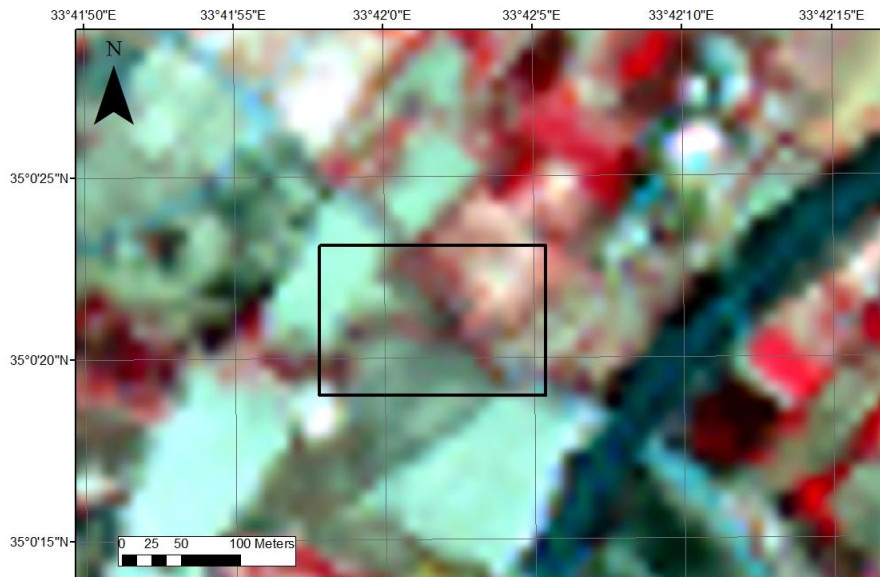


Figure 11: ALOS AVNIR-2 satellite image over the Pyla area in central Cyprus. The leakage is shown in the square.



Figure 12: QuickBird satellite image over the Pyla area in central Cyprus. The leakage is shown as a linear vegetated area in the centre of the image (indicated with arrow).

#### 4. DISCUSSION

The detection of water leakages using traditional techniques can be problematic especially in inaccessible areas. Remote sensing techniques can be used as a systematic tool for monitoring urban leakages. Remote sensing images may be used as an early warning system for the detection of problematic areas. In this paper an extensive field campaign took place in order to establish a spectral signature library for three typical targets (vegetation; soil and asphalt) under different moisture levels. Such spectral signatures may be used for any type of sensor after the necessary post-processing (e.g. RSR filters) covering the visible and very near infrared part of the spectrum.

The results have revealed the spectral behaviour of all different targets. Areas covered by soil or asphalt can be easily detected in real time since a slight increase of moisture affects the reflectance of the area. In addition, several VIs may be used for this purpose. The detection of leakages under vegetated areas seems to be problematic since no significant change of reflectance values was recorded. However, in cases where the satellite passes after a short period after the leakage event, fluctuations to vegetation spectral response can be observed in this area. Such detection is evident using both high and medium resolution satellite images.

#### ACKNOWLEDGEMENTS

The results reported here are based on findings of the Cyprus Research Promotion Foundation project “ΑΕΙΦΟΡΙΑ/ΦΥΣΗ/0311(BIE)/21”: Integrated use of space, geophysical and hyperspectral technologies intended for monitoring water leakages in water supply networks in Cyprus. The project is funded by the Republic of Cyprus and the European Regional Development Funds. Thanks are also given to the Remote Sensing Laboratory of the Department of Civil Engineering & Geomatics at the Cyprus University of Technology for its continuous support (<http://www.cut.ac.cy>).

## REFERENCES

- [1] Vairavamoorthy, K. and Lumbers, J., "Leakage Reduction in Water Distribution Systems: Optimal Valve Control", *J. Hydraul. Eng.*, 124(11), 1146–1154 (1998).
- [2] Pickerill, J. M. Malthus, T. J., "Leak detection from rural aqueducts using airborne remote sensing techniques, International", *Journal of Remote Sensing*, 19(12), 2427-2433 (1998).
- [3] Bastiaanssen, W.G.M., Brito, Bos M.G., Souza K.A., Cavalcanti E.B. and Bakker M.M., "Low cost satellite data for monthly irrigation performance monitoring", *Irrigation and Drainage systems*, 15, 53-79 (1998),
- [4] Schultz, G. and Engman, E., Present use and future perspective of remote sensing in hydrology and water management, In *Remote sensing and hydrology*, 545-551 (2001).
- [5] Tasumi, M., Trezza R., Allen R., and Wright J., "Validation tests on the SEBAL Model for evapotranspiration via satellite", *ICID Workshop on Remote sensing of ET* (2003)
- [6] Agapiou, A., Toullos, L., Themistocleous, K., Perdikou ,S., Alexakis, D.D., Sarris, A., Toullos, G., Clayton, C., Foinikaridou, H., Manolis, A. and Hadjimitsis, D.G., "Use of satellite derived vegetation indices for the detection of water pipeline leakages in semiarid areas", *Proc. First International Conference on Remote Sensing and Geoinformation*, 8-10 April 2013, Paphos, Cyprus (in press).
- [7] Agapiou, A., Hadjimitsis, D. G., Sarris, A., Georgopoulos, A. and Alexakis, D. D., "Optimum Temporal and Spectral Window for Monitoring Crop Marks over Archaeological Remains in the Mediterranean region", *Journal of Archaeological Science*, 40 (3), 1479–1492, doi: 10.1016/j.jas.2012.10.036 (2013)
- [8] Wu, X.; Sullivan, T.J. and Heidinger, K.A., "Operational calibration of the advanced very high resolution radiometer (AVHRR) visible and near-infrared channels", *Canadian Journal of Remote Sensing*, 36 (5), 602-616 (2010).
- [9] Agapiou, A, Hadjimitsis, DG and Alexakis, DD., "Evaluation of Broadband and Narrowband Vegetation Indices for the Identification of Archaeological Crop Marks", *Remote Sensing*. 4(12), 3892-3919 (2012).